Volume 51 • January 2013

ISSN 0008-6223

ELSEVIER

Carbon

an international journal

Reporting research on Carbonaceous Materials, their Production, Properties and Applications

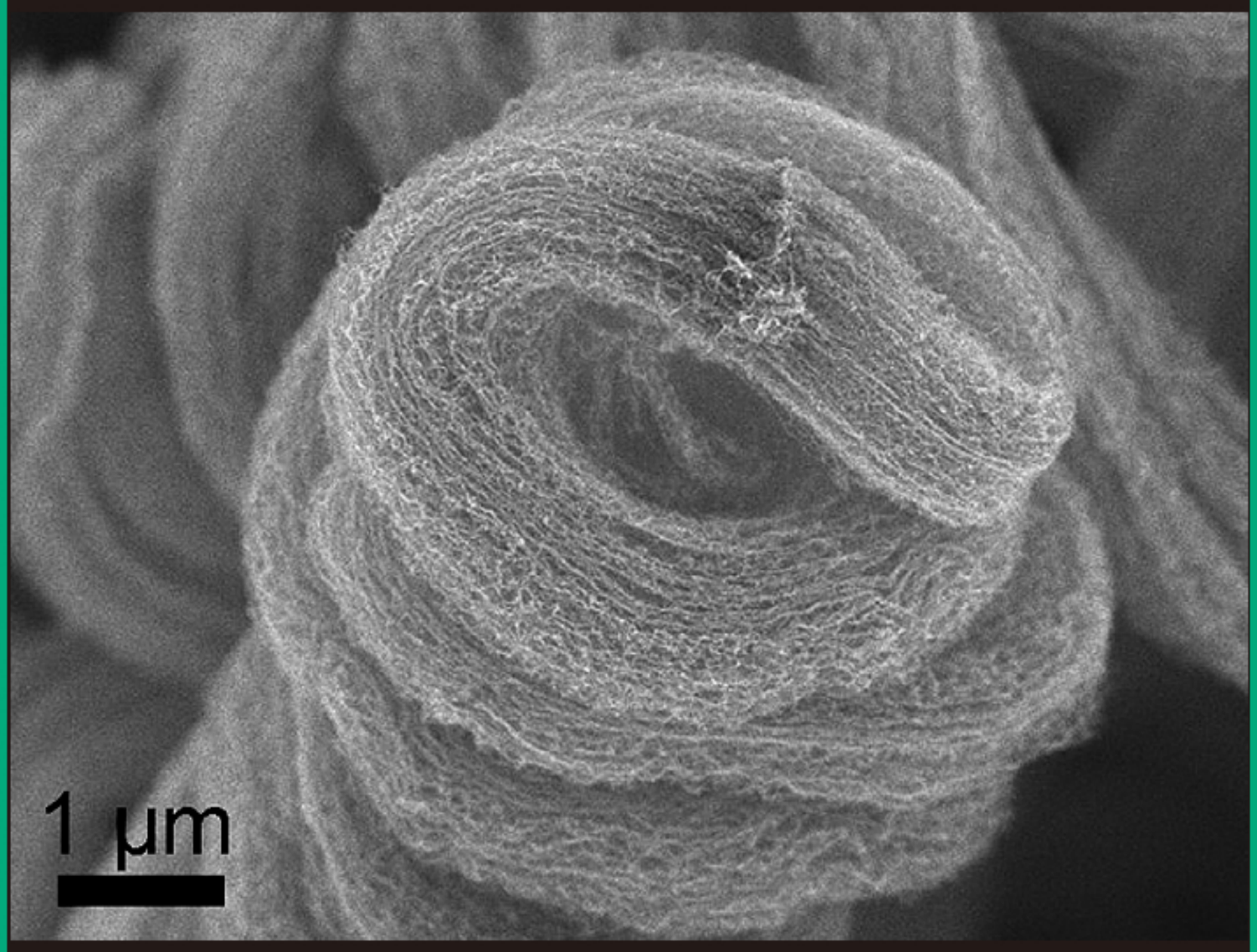

Editor-in-Chief: P.A. Thrower

Available online at www.sciencedirect.com

SciVerse ScienceDirect

51 Carbon Volume 51 • January 2013

ISSN 0008-6223

ELSEVIER

CARBON 50 (2012) 5323–5330

Available at www.sciencedirect.com

SciVerse ScienceDirect

journal homepage: www.elsevier.com/locate/carbon

Self-organization of nitrogen-doped carbon nanotubes into double-helix structures

*Gui-Li Tian, Meng-Qiang Zhao, Qiang Zhang *, Jia-Qi Huang, Fei Wei **

Beijing Key Laboratory of Green Chemical Reaction Engineering and Technology, Department of Chemical Engineering, Tsinghua University, Beijing 100084, China

ARTICLE INFO

Article history:
Received 14 May 2012
Accepted 11 July 2012
Available online 20 July 2012

ABSTRACT

Self-organization of nitrogen-doped carbon nanotube (N-CNT) double helices was achieved by chemical vapor deposition (CVD) with Fe–Mg–Al layered double hydroxides (LDHs) as the catalyst precursor. The as-obtained N-CNT double helix exhibited a closely packed nanostructure with a catalyst flake on the tip, which connected the two CNT strands on both sides of the flake. A mechanism for the self-organization of N-CNTs into double-helix structures with a moving catalyst head is proposed. Effective carbon/nitrogen sources, high-density active catalyst nanoparticles, space confinement, and the precise chiral match between the two CNT strands are found to be crucial for the N-CNT double helix formation. The morphologies of N-CNTs can be well tuned between bamboo-like and cup-stacked structures, and a CNT/N-CNT heterojunction can be constructed by changing the carbon feedstock from C_2H_4 to CH_3CN during CVD growth. N-CNT double helices with a length of 10–36 μm, a screw pitch of 1–2 μm, a CNT diameter of 6–10 nm, and a N-content of 2.59 at.% can be synthesized on the LDH catalysts by the efficient CVD growth.

1. Introduction

The diverse applications of carbon nanotubes (CNTs) in the area of materials, catalysis, energy storage, and biology science are interlinked not only to their superior physical properties, such as electric and thermal conductivity, but also to their chemical characters, such as functional groups, doping, and surface modification. The chemical property of CNTs can be easily tailored by heteroatom functionalization on nanocarbon sheets or molecular carbon geometries at the edges, defects, or strained regions, etc. Hitherto, great efforts have been devoted to develop heteroatom incorporated CNTs (such as B [1], N [1,2], O [3], P [4]) and the results show that the electronic properties of the sp^2 carbon can be tuned and hence give rise to their significantly improved catalytic activities and electrochemical performances. Therefore, the heteroatom incorporated CNTs are regarded as advanced materials in electrochemical energy storage [5], in catalyst supports for aerobic oxidation [6] and ammonia decomposition [7], and in metal-free catalysts for various reactions such as oxygen reduction reaction in fuel cell [8], triglyceride transesterification in biomass conversion [9,10], selective oxidation of H_2S [11], oxidative dehydrogenation, alkane activation reactions [12], etc.

Among various heteroatoms involved in CNTs, N is a unique element that bears five valence electrons. A shift in the Fermi level to the conducting band is presented when N is doped in carbon lattice as electron donors. With the incorporation of N into the nanocarbon framework, the reactivity of CNTs for oxygen reduction [8] or pseudo-capacitance [13] is introduced on carbon surface. The N-doped CNTs (N-CNTs) hence exhibit superior capacitance when used as electrode materials. Thus, exploring N-CNTs with controllable doping manner and tailored microstructures is scientifically necessary to demonstrate the material

* *Corresponding authors:* Fax: +86 10 6277 2051.
E-mail addresses: zhang-qiang@mails.tsinghua.edu.cn (Q. Zhang), wf-dce@tsinghua.edu.cn (F. Wei).
0008-6223/$ - see front matter
http://dx.doi.org/10.1016/j.carbon.2012.07.022

chemistry and potential applications of heteroatom-doped CNTs, as well as to allow mechanistic insight into the roles heteroatoms played for their textures and activities.

Generally, nitrogen and carbon sources are required for N-CNT formation. Various kinds of nitrogen-containing compounds, such as NH_3 [7], pyridine [14,15], acetonitrile [16], melamine [17], and benzylamine [18] have been selected as nitrogen sources for the chemical vapor deposition (CVD) growth of N-CNTs. However, the N-CNTs grown on granular catalysts were always strongly entangled to form agglomerates. When the synthesis of N-CNTs is performed on flat substrates (such as Si wafer, quartz plate, etc.), N-CNTs with good alignment and extraordinary properties are available [15,16,19]. Recently, large-scale intercalated growth of N-CNTs on natural clay was realized in a fluidized bed reactor [20]. The as-obtained three-dimensional N-CNTs serve as novel platforms to understand the dopant-induced perturbations and found wide applications in catalysis, electrochemistry, energy conversion and storages.

In this contribution, we report the efficient synthesis of N-CNT double helices by CVD growth on a layered double hydroxide (LDH) flake. The double-helix structure, which is the basic structure of deoxyribonucleic acid (DNA), is one of the most ubiquitous geometries that can be widely observed in nature, science, as well as human art and architectures [21,22]. Very recently, CNT arrays with double helical nanostructure were obtained among the CVD-grown products [23,24]. The CNT double helix provides a structural platform towards the design of hierarchical materials that can be used in areas such as nanoelectronics, magnetic devices, catalysis, separation, and energy conversion. To increase the reactivity of CNTs in the double helix, the synthesis of N-CNTs with double-helix structure by CVD was investigated. The growth behavior, structure, and formation mechanism of N-CNT double helices were also explored.

2. Experimental

2.1. Catalyst preparation

The Fe–Mg–Al LDH flakes were synthesized using a urea assisted co-precipitation reaction similar to our previous reports [23]. $Mg(NO_3)_2{\bullet}6H_2O$, $Al(NO_3)_3{\bullet}9H_2O$, and $Fe(NO_3)_3{\bullet}9H_2O$ were dissolved in 250.0 mL deionized water with $[Mg^{2+}]+[Al^{3+}]+[Fe^{3+}]$ = 0.19 mol/L, n(Mg): n(Al): n(Fe) = 2: 1: 0.8. The urea was then dissolved in the solution with molar concentration [urea] = 3.0 mol/L. The as-obtained solution was kept at 100 °C under continuous magnetic stirring for 9.0 h in a 500.0 mL flask, which was equipped with a reflux condenser in ambient atmosphere. The as-obtained suspension was kept at 94 °C for another 12 h without stirring. After filtering, washing and freeze-drying, the final products of Fe–Mg–Al LDH catalysts were available.

2.2. Synthesis of N-CNT double helices

The N-CNT double helices were prepared using a CVD method with Fe–Mg–Al LDH flakes as the catalyst precursor and ethylene/acetonitrile as carbon/nitrogen feedstocks. In the catalytic CVD growth, about 20 mg LDH catalysts were uniformly distributed on a quartz boat which was placed at the center of a horizontal quartz tube (inner diameter of 25 mm). The reactor was then inserted into a furnace at atmosphere pressure. The furnace was heated to 750 °C in Ar atmosphere at a flow rate of 115 mL/min. When reaching the reaction temperature, the mixed gas (H_2/C_2H_4) was introduced into the reactor with a flow rate of 25/20 mL/min. The CH_3CN was fed into the quartz reactor by a syringe pump with a feed rate of 3 mL/h simultaneously. The CVD growth was maintained for 1 h at 750 °C before the furnace was cooled to room temperature under Ar protection. The as-grown products were then collected for further characterization. In the controlled CVD growth, either C_2H_4 or CH_3CN was introduced for un-doped or doped CNT formation. In order to further investigate the effect of feedstock on the N-CNT double helix formation, in the control experimental Test 1, C_2H_4 was introduced firstly for 30 min, which was switched to CH_3CN for another 30 min subsequently, while in Test 2, the CH_3CN was introduced into the system before C_2H_4 and the duration for each growth period was also 30 min. In each experiment, H_2 was introduced as the reduction agent at the same time with the introduction of C_2H_4 or CH_3CN.

2.3. Characterizations

The morphology of the LDH flakes and the as-grown CNT products were characterized by a JSM 7401F scanning electron microscope (SEM) operated at 3.0 kV and a JEM 2010 high-resolution transmission electron microscope (TEM) operated at 120.0 kV. The samples for TEM observation were prepared using a routine sonication method with ethanol as the solvent. The Raman spectra were collected with a Renishaw RM2000 Raman spectrophotometer. He–Ne laser excitation line at 632.8 nm was employed to excite the Raman spectra. The purities of CNTs and N-CNTs in the as-grown product were obtained through thermogravimetric analysis (TGA) by Mettler Toledo TGA/DSC-1. The content of N element and the composition of N-containing functional groups were determined using X-ray photoelectron spectroscopy (XPS) by Escalab 250xi.

3. Results and discussion

The Fe–Mg–Al LDHs were employed as the catalyst precursor for the growth of CNTs and N-CNTs. LDHs are a class of synthetic two-dimensional nanostructured anionic clays, in which most metals (such as Mg, Al, Fe, Co, Ni, Cu, etc.) can be dispersed on the atomic scale with controllable component. Embedded metal particles with highly controllable density and particle size were available for the synthesis of aligned CNTwith this kind of catalysts [25,26]. In this contribution, a large amount of Fe–Mg–Al LDH agglomerates were served as the substrate and catalyst precursor, and they were firstly calcined into layered double oxide (LDO) flakes during the heating process. The Fe catalyst nanoparticles with a size ranging from 6.96 to 21.88 nm and a density of *ca.* $1.5 \times 10^{15}/m^2$ were formed and embedded on the LDO flakes after the reduction. With the introduction of C_2H_4 and CH_3CN, aligned N-CNTs with high density synchronously grew perpendicularly

to the Fe–Mg–Al LDO flakes. The two aligned N-CNT stands preferred to coil with each other when they met space resistance to release the pristine stress accumulated during the CNT deposition [27]. As shown in Fig. 1a, a large amount of double helices are observed to extend from the catalyst agglomerates. The as-obtained N-CNT double helices exhibit a closely packed structure with the LDO flakes on the tip, which connect the two N-CNT strands on both sides (Fig. 1b). The inserted figure in Fig. 1b indicates the N-CNTs in the strands offered good alignment. Fig. 1c–e illustrate the TEM images of the CNTs in the double-helix structures. The red arrow in Fig. 1c points out the LDO flake which maintains its flake morphology at high temperature. The N-CNTs are with bamboo-like structure and their diameters are measured as *ca*. 10 nm (Fig. 1e).

XPS technique was employed to determine the content of N element and the relative ratios of different N-containing functional groups in the double helical N-CNTs. The N content in the as-grown N-CNT double helices was analyzed as 2.59 at.%. Fig. 2a shows the fine scan of N1s region in the XPS spectrum. The relative amounts of the pyridinic N (398.4 eV), pyrrolic N (400.1 eV), quaternary N (coordinated N atoms substituting C atoms in the graphene layers, 401.2 eV), oxidized N (402.9 eV), and chemisorbed N (404.8 eV) [20,28] in the N-CNT double helices were determined to be 11.7, 11.4, 34.8, 8.8, and 33.3 at.% by the peak area, respectively. The Raman spectrum shown in Fig. 2b is presented to identify the graphitization degree of the N-CNT double helices. The intensity ratio of G band to D band is determined to be 0.84, showing a low graphitization degree of the N-CNT double helices. The low graphitization degree can be attributed to the substitution of C atoms by N atoms and also the pentagon-heptagon topological defects in the twisted N-CNTs. The thermogravimetric (TG) and differential thermogravimetric (DTG) curves of the N-CNT double helices in Fig. 2c show a sharp loss of mass to 3.04% with a peak position at around 451 °C, which is much lower than that of the un-doped CNT-array double helices at around 565 °C (Table 1). This indicates the introduction of N atoms into the CNT-array double helices significantly reduces their thermal stability. The yield of N-CNT double helices is 31.9 $g_{N\text{-}CNT}/g_{cat.}h$ according to the TGA results, which is much higher than traditional granular catalysts for agglomerated CNTs.

Both C_2H_4 and CH_3CN are highly required for N-CNT self-organized into double-helix structures. In one aspect, if only C_2H_4, without CH_3CN, was introduced into the CVD system,

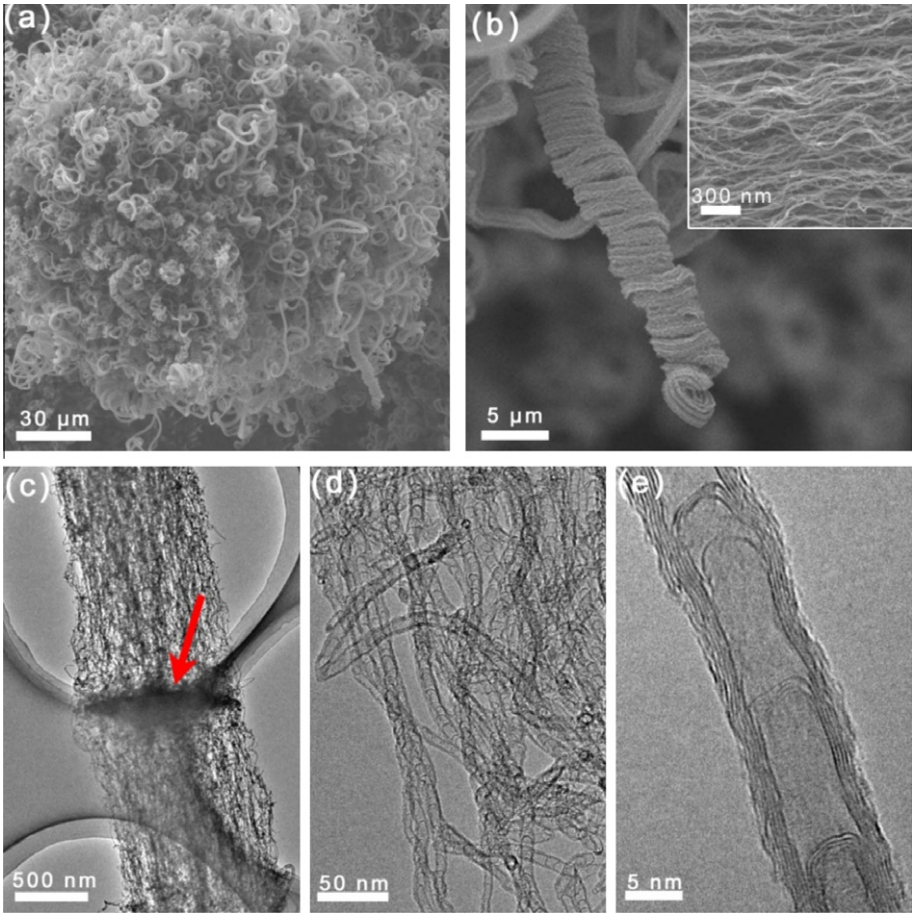

Fig. 1 – (a) The low and (b) high magnification SEM images of the as-obtained N-CNT double helices; the inserted figure in (b) shows the alignment of the N-CNTs; (c–e) TEM images of the as-obtained N-CNT double helices. The red arrow in (c) points out the LDO flake. (For interpretation of the references to colour in this figure legend, the reader is referred to the web version of this article.)

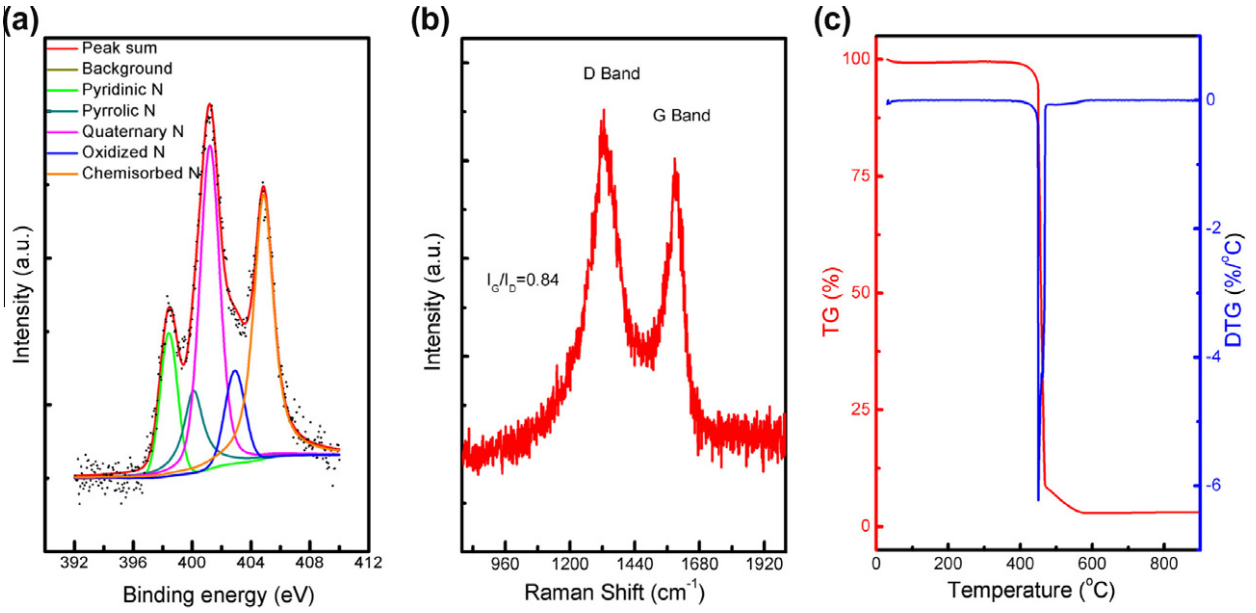

Fig. 2 – (a) The XPS spectra in N region; (b) Raman spectrum, (c) the TG and DTG curves for N-CNT double helices with co-feeding of C_2H_4 and CH_3CN.

Table 1 – A summary of CNT products grown on the Fe–Mg–Al LDH flakes.

Synthesis	Yield ($g_{CNT}/g_{cat.}$)	Total N content (at.%)	The ratio of N-functional groups (at.%)					DTG peak position (°C)
			Pyridinic N	Pyrrolic N	Quaternary N	Oxidized N	Chemisorbed N	
C_2H_4 and CH_3CN	31.9	2.59	0.304	0.295	0.901	0.227	0.863	451
C_2H_4 only	65.2	0	–		–	–	–	565
CH_3CN only	21.3	5.52	1.012	0.670	1.046	0.374	2.418	405
pre-C_2H_4, post-CH_3CN	63.1	0.22	0.049	0.047	0.020	0.044	0.060	563
pre-CH_3CN, post-C_2H_4	30.3	2.24	0.348	0.195	0.660	0.203	0.834	433

un-doped CNT-array double helices were fabricated (Fig. 3a–c). The CNT double helices grown with C_2H_4 alone as the carbon source were much longer, several hundred micrometers generally, and CNTs in double helices tightly compacted with each other (seen in the inserted figure of Fig. 3a). In another aspect, when CH_3CN, instead of C_2H_4, served alone as reaction precursor, the as-obtained CNT products were mainly short aligned CNTs with a length of several micrometers (Fig. 3d–f). The typical morphology of the short aligned CNTs was presented as Fig. 3d and the red arrows pointed out the LDO flakes. Compared with the CNT arrays shown in Fig. 3a, very sparse short aligned N-CNTs were presented in the inserted SEM image of Fig. 3d. Fig. 3b and e illustrated the TEM images of the long CNT-array double helices and the short aligned N-CNTs. The un-doped CNTs in the double helices were with hollow inner core and small diameters of *ca.* 8 nm. In contrast, the N-doped short aligned CNTs were with cup-stacked morphology and much larger diameters of *ca.* 20 nm. The XPS spectra of the nitrogen region in Fig. 3c and f reveal the sorts and relative proportions of different N-containing functional groups. The CNTs in the double helices produced with C_2H_4 were un-doped, while the nitrogen content in the short aligned CNTs produced with CH_3CN was with a high value of 5.52 at.%. The relative ratios of chemisorbed N, quaternary N, pyridinic N, pyrrolic N, and oxidized N were 43.8, 19.0, 18.3, 12.1, and 6.8 at.%, respectively.

In order to further investigate the effect of C_2H_4 and CH_3CN on the formation of N-CNT double helices, two control experimental tests with C_2H_4 and CH_3CN introduced into the system alternatively were carried out. In Test 1, C_2H_4 was introduced into the system first for the CVD growth of CNTs, which was switched to CH_3CN subsequently. The as-obtained products were CNTs in double helical structure, as shown in Fig. 4a. In contrast, for Test 2, CH_3CN was introduced into the system before C_2H_4. Fig. 4b shows the SEM image of the as-produced CNTs, which were in short-aligned structure with the lengths of several micrometers. Fig. 4c–f showed the TEM images of the two kinds of CNT products. The CNTs in the double helices with C_2H_4 as the initial feedstock were mainly hollow CNTs. However, it was observed that the interchange of carbon and nitrogen sources caused the formation of un-doped/doped CNT heterojunctions, as shown in Fig. 4e. Meanwhile, cup-stacked CNTs were the main product when CH_3CN was the initial feedstock. Fig. 5a provides the fine scan of XPS spectra in N region of CNT products in Test 1 and the content of doped N was determined to be 0.22 at.%, while

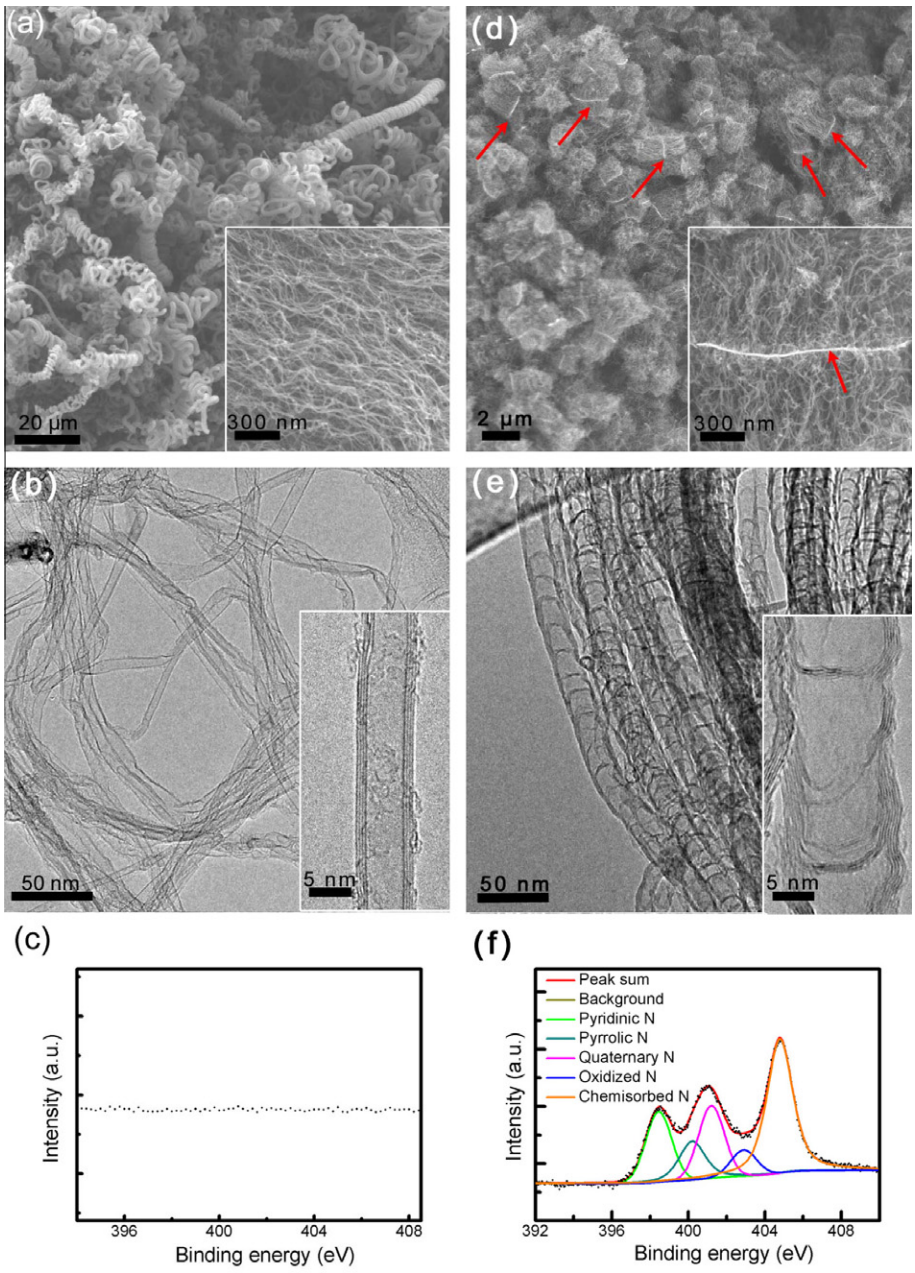

Fig. 3 – (a) The SEM images, (b) the TEM images and (c) the XPS curve in N region of un-doped CNT double helices with C_2H_4 as feedstock; and (d) the SEM images, (e) the TEM images and (f) the XPS curve in N region of short aligned N-doped CNTs with CH_3CN as feedstock. Inserts in (a–d) show corresponding high magnification SEM and TEM images of the samples.

the content of doped N in the short aligned CNTs synthesized in Test 2 was much higher (*ca.* 2.24 at.%, as shown in Fig. 5b). The chemisorbed N, quaternary N, pyridinic N, oxidized N, and pyrrolic N were with the relative atom ratios 37.2, 29.5, 15.5, 9.1, and 8.7 at.%, respectively. Fig. 5c and d provide the TG and DTG curves of the N-CNT products in Test 1 and 2. The TG curve of the sample in Test 1 showed a sharp mass loss to 1.56% with the position of weight loss peak at 563 °C. Meanwhile, the TG curve of N-CNT sample in Test 2 showed a residual mass ratio 3.19% with the position of weight loss peak at 433 °C. The CNT yields were 63.1 and 30.3 $g_{CNT}/g_{cat.}$ for Test 1 and 2, respectively. A summary of the structure, yield, and the amounts of nitrogen-containing functional groups in the above mentioned products were presented in Table 1.

Based on the experimental results, the mechanism for the self-organization of N-CNT double-helix structures during CVD growth is proposed as follows. With the introduction of C_2H_4 alone as the carbon source, CNTs are deposited on the Fe catalyst nanoparticles embedded on the LDO flakes with hollow inner cores. In contrast, with the only introduction of CH_3CN, the N atoms bearing five valence electrons easily absorb on the metal surface and block the hydrocarbon cracking and sp^2 carbon precipitation. Therefore, the formation rate of sp^2 carbon decreases and the continuous precipitation of graphene layer for the outer wall of N-CNTs are disturbed.

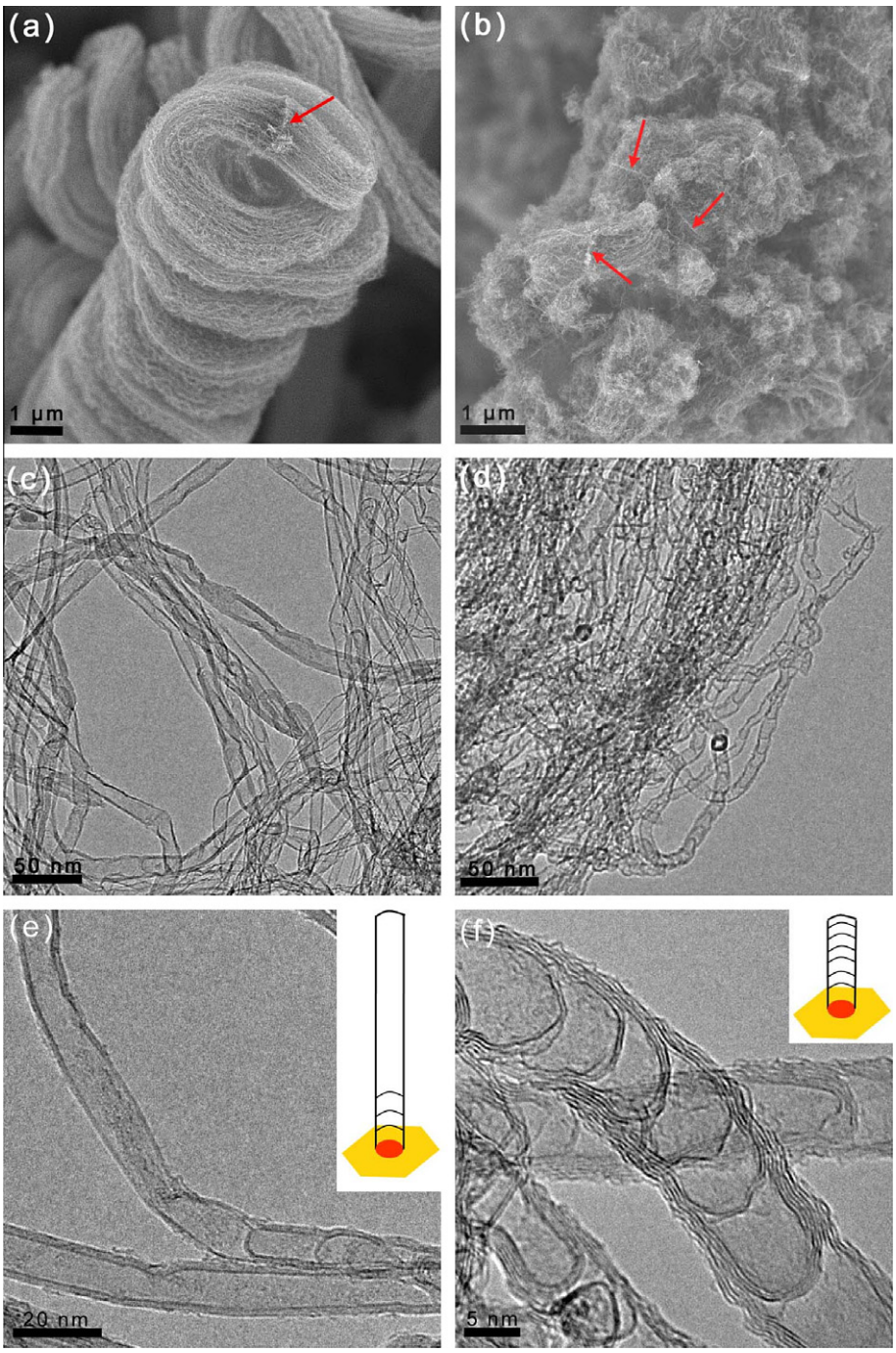

Fig. 4 – The SEM images and TEM images of (a, c, e) N-CNT double helices with pre-C_2H_4-post-CH_3CN as the carbon/nitrogen source and (b, d, f) the as-obtained short aligned N-CNT with pre-CH_3CN-post-C_2H_4 as the carbon/nitrogen source. The figure (e) shows a CNT/N-CNT heterojunction. The inserted illustrations in (e) and (f) show the alternate growth of CNT and N-CNT with alternate feedstock.

Cup-stacked N-CNTs, instead of standard graphitic walled CNTs are therefore formed (as shown in Fig. 3e). The active site of the CNT formation is at the interface of CNT/LDO flake, which is the so-called 'root growth' for aligned CNT synthesis in a heterogeneous catalysis process [23]. As a result, in Test 1, the pre-introduced C_2H_4 gave rise to the fast growth of standard CNTs with hollow structure and formed the double-helix structure. The cup-stacked CNTs were grown out on the same catalyst with much lower precipitation rate when CH_3CN was introduced instead of C_2H_4. Thus, a full carbon heterojunction with CNT/N-CNT interconnect was available in the double-helix products in Test 1. In contrast, the cup-stacked CNTs were firstly synthesized with pre-introduction of CH_3CN with low activities of Fe catalyst particles. Even when the carbon

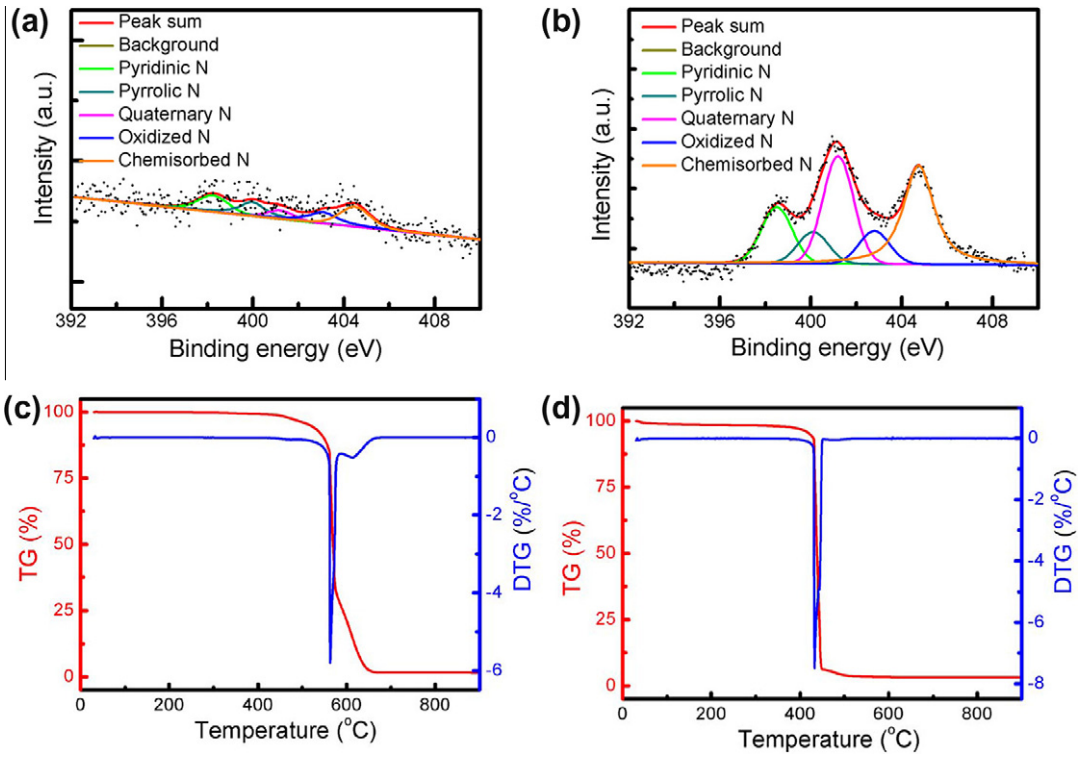

Fig. 5 – The XPS spectra in N region, the TG and DTG curves of (a and c) N-CNT double helices with pre-C_2H_4-post-CH_3CN as the carbon/nitrogen source and (b and d) the as-obtained short aligned N-CNT with pre-CH_3CN-post-C_2H_4 as the feedstock, respectively.

sources were switched to C_2H_4, the catalytic activity cannot be fully recovered, and as results, short but highly doped CNT products were synthesized.

Only the co-feeding of CH_3CN and C_2H_4 can lead to the formation of N-CNT double helices with a bamboo structure and high N-doped value. This is attributed to the good catalytic activities of Fe catalysts for continuous precipitation of sp^2 carbon for the formation of N-CNT outer layers. Meanwhile, compared with sole CH_3CN as feedstock, the co-feeding of CH_3CN and C_2H_4 prevents the deactivation of catalyst particles effectively. The CNT is a typical kind of chiral nanomaterial. During the CVD growth, it is shown that both the SWCNTs and MWCNTs render a small-angle rotation misorientation between adjacent sections along the catalyst nanoparticles, indicating the CNTs exert stresses that rotate, twist, and bend small section of the catalyst during CVD growth [29,30]. Herein the N-CNTs were synchronously grown from the LDO flake with internal rotation stress which arises from the rotation of individual N-CNT impeded by neighboring N-CNTs in the strand. The defect induced by N atom doping gives the defects and some rotation stress maybe released. When two CNT stands oppositely grow on a flake with their tips under space resistance (such as other CNT strands, catalysts, or substrates), the N-CNTs with the same handness prefer to coil themselves into N-CNT double helix to release the rotation stress [27]. Whether the CNT strand or double helix is left or right handed is not fully understood yet. Nevertheless, it was demonstrated that two left-handed N-CNTs strands connected by a catalyst node lead to the formation of a right-handed double helix, while self-organization of two right-handed N-CNT strands gives the left-handed double helix. In general, the N-CNT double helix growth requires effective carbon and nitrogen sources, high density of active catalyst nanoparticles, space confinement, and the precise match between the two CNT strands.

4. Conclusions

The self-organization of N-CNT double-helix structures with a moving catalyst head has been realized by CVD growth using Fe–Mg–Al-LDH catalyst. The N-CNT double helices with a length of 10–36 μm, a screw pitch of 1–2 μm, a CNT diameter of 6–10 nm, and a N-content of 2.59 at.% were synthesized by efficient CVD growth on the LDH catalysts. The cup-stacked or bamboo-like N-CNTs were selectively synthesized on Fe nanoparticles with controllable carbon source. When only CH_3CN is introduced, the sp^2 carbon formation rates decrease and the continuous precipitation of sp^2 graphene layer for the outer wall of N-CNTs becomes difficult, leading to the formation of cup-stacked N-CNTs. A full carbon heterojunction with CNT/N-CNT interconnect was constructed with subsequently introduction of C_2H_4 and CH_3CN. The co-feeding of CH_3CN and C_2H_4 can give rise to the formation of N-CNT double helices with a bamboo-like structure. The carbon/nitrogen sources, high density of active catalyst nanoparticles, space confinement, and the chiral match between the two CNT strands are the prerequisites for the formation of N-CNT double helices. These results not only provide new insights on N-CNT formation with tunable structures, but also shed some light on the formation mechanism of CNT double

helices and their potential applications in the area of heterogeneous catalysis, energy storage, biology, composite, and nanoelectronics.

Acknowledgements

The work was supported by the Foundation for the China National Program (No. 2011CB932602) and the Natural Scientific Foundation of China (No. 20736004).

REFERENCES

[1] Wang B, Ma YF, Wu YP, Li N, Huang Y, Chen YS. Direct and large scale electric arc discharge synthesis of boron and nitrogen doped single-walled carbon nanotubes and their electronic properties. Carbon 2009;47(8):2112–5.
[2] Ayala P, Arenal R, Rummeli M, Rubio A, Pichler T. The doping of carbon nanotubes with nitrogen and their potential applications. Carbon 2010;48(3):575–86.
[3] Xia W, Yin XL, Kundu S, Sanchez M, Birkner A, Woll C, et al. Visualization and functions of surface defects on carbon nanotubes created by catalytic etching. Carbon 2011;49(1):299–305.
[4] Zhang J, Liu X, Blume R, Zhang AH, Schlogl R, Su DS. Surface-modified carbon nanotubes catalyze oxidative dehydrogenation of *n*-butane. Science 2008;322(5898):73–7.
[5] Bulusheva LG, Okotrub AV, Kurenya AG, Zhang HK, Zhang HJ, Chen XH, et al. Electrochemical properties of nitrogen-doped carbon nanotube anode in li-ion batteries. Carbon 2011;49(12):4013–23.
[6] Yu H, Peng F, Tan J, Hu XW, Wang HJ, Yang JA, et al. Selective catalysis of the aerobic oxidation of cyclohexane in the liquid phase by carbon nanotubes. Angew Chem Int Ed 2011;50(17):3978–82.
[7] Garcia-Garcia FR, Alvarez-Rodriguez J, Rodriguez-Ramos I, Guerrero-Ruiz A. The use of carbon nanotubes with and without nitrogen doping as support for ruthenium catalysts in the ammonia decomposition reaction. Carbon 2010;48(1):267–76.
[8] Masa J, Bordoloi A, Muhler M, Schuhmann W, Xia W. Enhanced electrocatalytic stability of platinum nanoparticles supported on a nitrogen-doped composite of carbon nanotubes and mesoporous titania under oxygen reduction conditions. ChemSusChem 2012;5(3):523–5.
[9] Tessonnier JP, Villa A, Majoulet O, Su DS, Schlogl R. Defect-mediated functionalization of carbon nanotubes as a route to design single-site basic heterogeneous catalysts for biomass conversion. Angew Chem Int Ed 2009;48(35):6543–6.
[10] Villa A, Tessonnier JP, Majoulet O, Su DS, Schlogl R. Transesterification of triglycerides using nitrogen-functionalized carbon nanotubes. ChemSusChem 2010;3(2):241–5.
[11] Chizari K, Deneuve A, Ersen O, Florea I, Liu Y, Edouard D, et al. Nitrogen-doped carbon nanotubes as a highly active metal-free catalyst for selective oxidation. ChemSusChem 2012;5(1):102–8.
[12] Su DS, Zhang J, Frank B, Thomas A, Wang XC, Paraknowitsch J, et al. Metal-free heterogeneous catalysis for sustainable chemistry. ChemSusChem 2010;3(2):169–80.
[13] Lota G, Fic K, Frackowiak E. Carbon nanotubes and their composites in electrochemical applications. Energy Environ Sci 2011;4(5):1592–605.
[14] Ilinich GN, Moroz BL, Rudina NA, Prosvirin IP, Bukhtiyarov VI. Growth of nitrogen-doped carbon nanotubes and fibers over a gold-on-alumina catalyst. Carbon 2012;50(3):1186–96.
[15] Xu EY, Wei JQ, Wang KL, Li Z, Gui XC, Jia Y, et al. Doped carbon nanotube array with a gradient of nitrogen concentration. Carbon 2010;48(11):3097–102.
[16] Cui TX, Lv RT, Huang ZH, Zhu HW, Zhang J, Li Z, et al. Synthesis of nitrogen-doped carbon thin films and their applications in solar cells. Carbon 2011;49(15):5022–8.
[17] Liu H, Zhang Y, Li RY, Sun XL, Desilets S, Abou-Rachid H, et al. Structural and morphological control of aligned nitrogen-doped carbon nanotubes. Carbon 2010;48(5):1498–507.
[18] Koos AA, Dillon F, Obraztsova EA, Crossley A, Grobert N. Comparison of structural changes in nitrogen and boron-doped multi-walled carbon nanotubes. Carbon 2010;48(11):3033–41.
[19] Lv RT, Cui TX, Jun MS, Zhang Q, Cao AY, Su DS, et al. Open-ended, n-doped carbon nanotube-graphene hybrid nanostructures as high-performance catalyst support. Adv Funct Mater 2011;21(5):999–1006.
[20] Huang JQ, Zhao MQ, Zhang Q, Nie JQ, Yao LD, Su DS, et al. Efficient synthesis of aligned nitrogen-doped carbon nanotubes in a fluidized-bed reactor. Catal Today 2012;186(1):83–92.
[21] Su DS. Inorganic materials with double-helix structures. Angew Chem Int Ed 2011;50(21):4747–50.
[22] Yang M, Kotov NA. Nanoscale helices from inorganic materials. J Mater Chem 2011;21(19):6775–92.
[23] Zhang Q, Zhao M-Q, Tang D-M, Li F, Huang J-Q, Liu B, et al. Carbon-nanotube-array double helices. Angew Chem Int Ed 2010;49(21):3642–5.
[24] Zhao M-Q, Huang J-Q, Zhang Q, Nie J-Q, Wei F. Stretchable single-walled carbon nanotube double helices derived from molybdenum-containing layered double hydroxides. Carbon 2011;49(6):2148–52.
[25] Zhao M-Q, Zhang Q, Zhang W, Huang J-Q, Zhang Y, Su DS, et al. Embedded high density metal nanoparticles with extraordinary thermal stability derived from guest-host mediated layered double hydroxides. J Am Chem Soc 2010;132(42):14739–41.
[26] Zhao M-Q, Zhang Q, Huang J-Q, Wei F. Hierarchical nanocomposites derived from nanocarbons and layered double hydroxides - properties, synthesis, and applications. Adv Funct Mater 2012;22(4):675–94.
[27] Zhao MQ, Zhang Q, Tian GL, Huang JQ, Wei F. Space confinement and rotation stress induced self-organization of double-helix nanostructure: a nanotube twist with a moving catalyst head. ACS Nano 2012;6(5):4520–9.
[28] Arrigo R, Havecker M, Wrabetz S, Blume R, Lerch M, McGregor J, et al. Tuning the acid/base properties of nanocarbons by functionalization via amination. J Am Chem Soc 2010;132(28):9616–30.
[29] Behr MJ, Mkhoyan KA, Aydil ES. Catalyst rotation, twisting, and bending during multiwall carbon nanotube growth. Carbon 2010;48(13):3840–5.
[30] Marchand M, Journet C, Guillot D, Benoit JM, Yakobson BI, Purcell ST. Growing a carbon nanotube atom by atom: “and yet it does turn”. Nano Lett 2009;9(8):2961–6.